Electron impact ionization of Ar^{10+}

A . Riahi , K . Laghdas, S . Rachafi
Département de Physique, Faculté des Sciences, Université Chouaib Doukkali, B.P. 20, 2400 ElJadida, Morocco.

Total and single differential cross sections have been calculated for electron impact ionization of Ar^{10+} ($1s^22s^22p^4$) $^3P^e$ using a method that combines the distorted-wave Born approximation and R-matrix theory. In this method, the incident/scattered electron is described by the distorted-wave Born approximation, while both the initial bound state and the final continuum states are expanded in terms of an R-matrix basis. Eight states of the final Ar^{11+} ion are considered, namely $1s^22s^22p^3\ ^4S^o\ ^2D^o\ ^2P^o$ and $1s^22s2p^4\ ^4P^e\ ^2D^e\ ^2S^e\ ^2P^e\ ^2P^o$.

Up to the 2^4- pole components of the interaction with ionizing electron were included, giving ten distinct Ar^{10+} continuum symmetries. We calculated single differential cross sections summed over final ionic states, as a function of the energy loss. These cross sections exhibit considerable structure due to autoionizing resonances. Total cross sections for production of Ar^{11+} in each of the eight states are presented for impact energies from threshold energy at 19.8 au to 200 au. Our theoretical values for the total cross section are in good agreement with recent experimental results.

I. INTRODUCTION

In fusion plasma research, as in astrophysics, a good knowledge of physical properties and collisional atomic data is needed in order to interpret the observations made of various plasma parameters. One of the fundamental processes in this field is the electron-impact ionization of atoms or ions [1], because it governs the relative proportions of the various ionization stages of each ion charge present in the plasma. The energetic radiation from highly ionized impurities in high-temperature plasmas is a major cause of energy loss which has so far prevented such devices from reaching the required ignition temperature $(KT \geq 10\,keV)$ and confinement condition $(n\tau \geq 10^{14} cm^{-3}.s)$. The effect of impurity ions on plasma confinement is also poorly understood.

For many years there has been considerable theoretical interest in electron impact ionization processes, motivated on the one hand by the need to develop reliable methods of calculating (for example) the ion charge state distribution in the plasma and the corresponding ionization cross sections, and on the other by the urgent practical need to obtain accurate data for plasma and fusion research [2].

For single ionization, theoretical results have been obtained using various applications of the Coulomb-Born approximations where both the incident and outgoing electrons are described by pure or distorted Coulomb or plane waves [3]. The fundamental problem here is the fact that in this type of calculation all correlations between the incident and outgoing electrons with the initial and final ionic states are completely neglected. On the experimental side, the information available regarding the electron impact ionization process has been analysed in detail [4] for a large number of targets of thermonuclear interest. Accurate models for plasmas require reliable cross section data for electron-impact excitation, ionization and recombination of these impurity ions.

In the present study, we have used the distorted-wave Born approximation (DWBA)-R-matrix method of Bartschat and Burke [5] to calculate total and single differential cross sections for electron-impact ionization. This method incorporates the indirect process of excitation-autoionization (EA) by treating the final continuum states (consisting of the final ion plus the ejected electron) by an accurate R-matrix formulation. The initial bound state of the target ion is also calculated by the R-matrix method and is thus consistent with the final continuum states.

In the R-matrix method the close-coupling [6] problem is solved for the inner region, $r \leq a$, subject to a fixed boundary condition at $r=a$ to give the basis functions. Wave functions for a system containing (N+1) electrons for any system energy can be expanded in terms of products of N-electrons residual ion functions multiplied by fully optimised functions for an ejected electron and matched to functions for the outer region $r > a$.

The advantage of the R-matrix method compared with the usual close-coupling approach [6] is the fact that a broad range of energies of the ejected electron can be studied by a single diagonalisation of the Hamiltonian matrix, instead of solving a system of coupled integrodifferential equations at each energy. Because the ‘ fast’ ionizing electron is described by the distorted-wave Born approximation we neglect all the correlations between this electron and the electrons of target. Exchange effects are approximated by modifying the range of integration over the energy of the ejected electron ‘ half range’.

The plan of this paper is as follows. In section 2 we present a broad general outline of the theory of the R-matrix method. More details can found in the paper of Bartschat and Burke [5]. Computational details of the method have been described by Bartschat [7]. Section 3 gives details of the specific calculation for Ar^{10+}. The results for single differential cross sections and total cross sections are presented, and compared with experiment, in section 4.

II. THE R-MATRIX METHOD OF IMPACT IONIZATION

A. GENERAL THEORY

Consider the problem of calculating the cross section for the electron-impact ionization of complex positive ions :

$$e_0^-(k_0) + X^{q+} \rightarrow \left[X^{q+}\right]^* + e_0^-(k_1) \quad \alpha \quad \left[X^{(q+1)+} + e_{N+1}^-(k_2)\right] \tag{1}$$

Here X^{q+} and $X^{(q+1)+}$ are the initial and final states of the ionic target, the asterisk on the $\left[X^{q+}\right]^*$ indicating formation of a continuum state. This continuum state represents the intermediate states of a (N+1)-electrons system for which N electrons are bound in an atomic ion represented by the final-ion state $X^{(q+1)+}$ and one electron e_{N+1}^- can escape to infinity with l_2 th partial wave. The ionization process can be resolved into partial waves. In the present work we describe this process using the following approximations :

- The ionizing electron $e_0^-(k_0)$ with initial and final momenta $\mathbf{k}_0$ and $\mathbf{k}_1$ is described by the distorted-wave Born approximation.
- e_{N+1}^- is a ejected electron with momenta $\mathbf{k}_2$ and the initial and final continuum (N+1) electron states Ψ_i and $\Psi_f^-\left\{X^{(q+1)+} + e_{N+1}^-(k_2)\right\}$ are calculated using the R-matrix approach. The process is treated in *LS* coupling where only Coulomb interaction between the ionizing electron and the target electrons is taken into account.

B. THE R-MATRIX EXPANSION

In this subsection we discuss the use of an R-matrix basis to represent the initial and final (N+1)-electron states. We start with a brief summary of the basic equations of the general R-matrix theory [8,9].

In the R-matrix method, the configuration space, describing the scattered or ejected electron and the target, can be separated into two distinct regions. The inner region is defined as that region enclosed by a sphere of radius '*a*' centred on the origin of the atomic system, and is chosen to be large enough to just envelop the charge distribution of the target states of interest.

The outer region consists of all other space and we can assume that in this region the target eigenstate is zero.

In this method , since the initial and final (N+1) electron states Ψ_i and Ψ_f are obtained by diagonalising the same target Hamiltonian H_{ion} [10,11,12], they are orthogonal. In the inner region, the wavefunction of the target can be expanded in terms of energy- independent R-matrix basis functions for any energy E :

$$\Psi_E = \sum_k A_{E_k} \psi_k \tag{2}$$

The R-matrix basis functions are defined by

$$\psi_k = A\sum_{ij} \Phi_i(\backslash r_{N+1}) r_{N+1}^{-1} u_{ij}(r_{N+1}) c_{ijk} + \sum_j d_{jk} \varphi_j(X_{N+1}) \tag{3}$$

Here $\Phi_i(\backslash r_{N+1})$ are channel functions formed by coupling a target state with the spin and angular components of the scattered electron, and are channel eigenstates of L and S respectively and of π of the system. $\backslash r_{N+1}$ means the inclusion of all coordinates except the radial coordinate of the $(N+1)^{th}$ electron, or writing generally,

$$\backslash r_i = \left\{X_1, \ldots, X_{i-1}, X_{i+1}, \ldots, X_{N+1}, \overline{\pi}_i, \sigma_i\right\} \tag{4}$$

A is the antisymmetrisation operator which ensures that the Pauli principe is satisfied.

The $\varphi_j(X_{N+1})$ are quadratically integrable correlation functions, which are short range and consist totally of bound configurations. Finally, u_{ij} are the R-matrix continuum orbitals which satisfy the differential equation :

$$\left(\frac{d^2}{dr^2} - \frac{l_i(l_i+1)}{r^2} + V_i(r) + k_i^2\right) u_{ij}(r) = \sum_n \lambda_{ij} p_{nl_i}(r) \tag{5}$$

for each angular momentum, l_i, subject to the R-martix boundary conditions

$$u_{ij}(0) = 0$$
$$\frac{a}{u_{ij}(a)} \frac{du_{ij}}{dr}\Big|_{r=a} = b \tag{6}$$

The logarithmic derivative *b* is usually taken to be zero and the R-matrix boundary a is chosen in such a way that all the bound orbitals $P_{nl_i}(r)$ used in the description of the channel and correlation functions essentially vanish for *r* > *a*. The λ_{ij} are Lagrange multipliers, and are chosen to ensure that the continuum orbitals are orthogonal within a particular symmetry to the bound orbitals $P_{nl_i}(r)$

In order to keep the notation compact the equation (3) can be write as :

$$\psi_k = \sum_{k'} \omega_{k'k} \phi_{k'} \tag{7}$$

The coefficients $\omega_{kk'}$, which correspond collectively to the c_{ijk} and d_{jk} in equation (3), are determined by diagonalising the (N+1)-electrons Hamiltonian as :

$$\sum_{k'k} \omega_{kk''} <\phi_k|\mathbf{H}|\phi_{k'}> \omega_{k'k'''} = E_{k''}\delta_{k''k'''} \qquad (8)$$

Both the initial and final (N+1)-electrons states are now expanded in terms of the R-matrix basis functions as follows :

$$\Psi_i = \sum_k A_{ki} \ \psi_k \qquad (9)$$

and

$$\Psi_f^- = \sum_k A_{kf}^- \ \psi_k \qquad (10)$$

In order to determine the coefficients A_{ki} and A_{Kf}^- it is necessary to calculate the radial wavefunctions of the continuum electron in the outer region. The complete solution can be obtained by matching the inner region and outer region wavefunctions at the boundary.

III. COMPUTATIONAL DETAILS

We have considered the ionization of Ar^{10+} in its ground state $(1s^2 2s^2 2p^4)\ ^3P^e$

$$e_0^-(E_0,\lambda_0) + Ar^{10+}(1s^2 2s^2 2p^4)^3P^e \rightarrow e_0^-(E_1,\lambda_1) + Ar^{10+}(\varepsilon^3 L^\pi) \qquad (11)$$

$$Ar^{10+}(\varepsilon^3 L^\pi) \rightarrow \begin{cases} Ar^{11+}(1s^2 2s^2 2p^3)^4S^o + e_{N+1}^-(E_2(^{2s+1}L_f), l_2) \\ Ar^{11+}(1s^2 2s^2 2p^3)^2D^o + e_{N+1}^-(E_2(^{2s+1}L_f), l_2) \\ Ar^{11+}(1s^2 2s^2 2p^3)^2P^o + e_{N+1}^-(E_2(^{2s+1}L_f), l_2) \\ Ar^{11+}(1s^2 2s2p^4)^4P^e + e_{N+1}^-(E_2(^{2s+1}L_f), l_2) \\ Ar^{11+}(1s^2 2s2p^4)^2D^e + e_{N+1}^-(E_2(^{2s+1}L_f), l_2) \\ Ar^{11+}(1s^2 2s2p^4)^2S^e + e_{N+1}^-(E_2(^{2s+1}L_f), l_2) \\ Ar^{11+}(1s^2 2s2p^4)^2P^e + e_{N+1}^-(E_2(^{2s+1}L_f), l_2) \\ Ar^{11+}(1s^2 2p^5)^2P^o + e_{N+1}^-(E_2(^{2s+1}L_f), l_2) \end{cases} \qquad (12)$$

Equation (11) shows the excitation of Ar^{10+} to continuum state of symmetry $(\varepsilon^3 L^\pi)$ caused by the 2^4-pole components of the interaction with the incident electron, $e_0^-(E_0, l_0)$ which has incident energy E_0 and angular momentum l_0. The electrostatic interaction between $e_0^-(E_0, l_0)$ and the N+1 electrons of Ar^{10+} causes $e_0^-(E_0, l_0)$ to lose energy $\Delta E = E_0 - E_1$ and excites Ar^{10+} from the ground state to a continuum state of symmetry $(\varepsilon^3 L^\pi)$. With an initial $^3P^e$ state ($L_0 = 1$), the final state symmetry is identified by $|\lambda - 1| \le L \le \lambda + 1$ and $\pi = (-1)^\lambda$. In practice, we have included only the interaction components with all $\lambda < 4$, and so ten continuum states are accessible, with symmetries: $^3P^e$, $^3S^o$, $^3P^o$, $^3D^o$, $^3D^e$, $^3F^e$, $^3F^o$, $^3G^o$ and $^3H^e$. We took an R-matrix radius of $1.984a_o$ and constructed radial continuum orbitals $u_{nl}(r)$ (n = 1,…10) for each angular momentum $l_2 = 0,\ldots,7$.

Equation (12) shows that, in the outer region, the continuum states consist of Ar^{11+} and an ejected electron, $e_{N+1}^-(E_2, l_2)$, with energy $E_2(^{2s+1}L_f)$ and angular momentum l_2. We have included the eight states with configurations $1s^2 2s^2 2p^3$, $1s^2 2s2p^4$ and $1s^2 2p^5$. The bound 1s, 2s and 2p radial orbitals from which the wavefunctions are constructed were obtained from those given by Clementi and Roetti [13] for $(1s^2 2s^2 2p^3)^4S^o$ reoptimized to the sum of the energies of the $(1s^2 2s^2 2p^3)^4S^o$, $^2D^o$, $^2P^o$ states using the CIV3 code [14]. Our calculated energy of the ground state of Ar^{11+} is –453.183051 au, which compares favourably with the value of –453.184020 au given by Clementi and Roetti [13] and is indicative of the quality of the wavefunction. The energy of the final continuum state of the Ar^{10+} system is characterised by the energy-loss ΔE :

$$\Delta E = E_0 - E_1 = E_2 + I(^{2s+1}L_f) \qquad (13)$$

where $I(^{2s+1}L_f)$ is the ionization potential relative to the initial bound state for production of the final ion in

each Ar^{11+}core. Since I($^{2s+1}L_f$) is fixed, the ionization is characterised by E_0 and ΔE .

IV. RESULTS

A. SINGLE DIFFERENTIAL CROSS SECTION

The single differential cross section for ionizing $(1s^2 2s^2 2p^4)^3P^e$ state of Ar^{10+} with production of the Ar^{11+} ion in the final state via continuum symmetry is given by :

$$\frac{d\sigma_f^L}{dE_2}(E_2,E_0)=\frac{16}{E_0(2L_0+1)}\sum_{l_0 l_1 l_2}\left|<\Psi_f^{(-)}\left\|\vartheta^{(L)}(\lambda_1 k_1 \lambda_0 k_0)\right\|\Psi_i>\right|^2 \tag{14}$$

with

$$\vartheta^{(L)}(\lambda_1 k_1 \lambda_0 k_0)=\sum_{i=1}^{N+1}\Re^{\lambda}_{\lambda_0\lambda_1}(k_0,k_1;r_i)\left(\frac{4\pi}{2\lambda+1}\right)^{\frac{1}{2}}Y_\lambda(\hat{r_i}) \tag{15}$$

where

$$\Re^{\lambda}_{\lambda_0\lambda_1}(k_0,k_1;r_i)=\left(\frac{(2\lambda_0+1)(2\lambda_1+1)}{2\lambda+1}\right)^{\frac{1}{2}}\begin{pmatrix}\lambda_0 & \lambda & \lambda_1\\ 0 & 0 & 0\end{pmatrix}\int_0^\infty \gamma_\lambda(r',r_i)F_{\lambda_0}(k_0,r')F_{\lambda_1}(k_1,r')dr' \tag{16}$$

where $\gamma_\lambda(r',r_i)=r_<^\lambda / r_>^{\lambda+1}$ are the lesser and greater of r' and r_i .

The functions $F_\lambda(k,r)$ are radial wavefunctions which are solutions of

$$\left(\frac{d^2}{dr^2}-\frac{\lambda(\lambda+1)}{r^2}+V(r)\right)F_\lambda(k,r)=0 \tag{17}$$

with

$$F_\lambda(k,0)=0 \tag{18}$$

$$F_\lambda(k,r)\approx_{r\to\infty}\frac{1}{\sqrt{k}}\sin\left(kr-\frac{1}{2}\lambda\pi+\frac{2Z}{k}\ln 2kr+\sigma_\lambda+\eta_\lambda\right)$$

where

$$\sigma_\lambda=\arg\Gamma\left(\lambda+1-\frac{iZ}{k}\right) \tag{19}$$

In equation (14), the operator $\vartheta^{(L)}(\lambda_1 k_1 \lambda_0 k_0)$ is proportional to the 2^λ-pole components of the interaction between e_0^- and the Ar^{10+} system overlapped between the λ_0 th and λ_1 th partial waves of e_0^- at energies of E_0 and E_1, respectively [5,6]. These partial waves were calculated using the static potential of $Ar^{10+}(1s^2 2s^2 2p^4)^3S^e$ obtained from the wavefunction given by Clementi and Roetti [13]. The maximum value of l_0 and l_1 that was sufficient to ensure convergence of the single differential cross section, ranged from $l'=14$ for E_0 = 22 au to $l''=66$ for E_0 = 180 au.

In figure l we present the single differential cross section for electron-impact ionization of

$Ar^{10+}(1s^2 2s^2 2p^4)^3P^e$ for impact energy E_0=50 au as a function of energy loss. Each contribution is from a particular continuum symmetry of Ar^{10+}, shown at the right margin, and is summed over the final states of Ar^{11+} . The cross section demonstrates the regular Rydberg series of resonances.

The resonances are due to quasibound autoionizing states consisting of an electron bound to an excited Ar^{11+} core such that the effective principal quantum number n^* is given by $n-\delta$ with n an integer and the quantum defect δ virtually constant for each series.

We have identified 43 distinct series of resonances, and table 2 shows the resonance energy ε_r and effective principal quantum number n^* for resonances with ($n<15$).

B. TOTAL CROSS SECTIONS

The total cross section for ionization that leaves the final ion in state f is :

$$\sigma_f(E_0)=\int_0^{\frac{E_0-I(l_f)}{2}}\frac{d\sigma_f}{dE}(E_2,E_0)dE_2 \tag{20}$$

where

$$\frac{d\sigma_f}{dE}(E_2,E_0)=\sum_L\frac{d\sigma_f^L}{dE}(E_2,E_0) \tag{21}$$

Here, the 'half-range' approximation is used in the integration over E_2 to take account of the indistinguishability of the two final, continuum electrons. The upper limit of ejected-electron energy E_2 is taken to be half of the maximum possible value $E_0 - I(L_f)$ [15].

Our calculated total cross sections are also presented in table 3 for impact energies from 20 au to 200 au. This table shows the total cross sections for electron-impact ionization of Ar^{10+} with production of Ar^{11+} in various states (columns 3-9). Column 2 ' σ_{Total} ' is the cross section summed over the states of Ar^{11+}. Figure 2 shows cross sections plotted for impact energies from threshold energy at 19.8 au to 200 au. In figure 3, we present the total cross section compared with the recent experimental results [16]. Our results are in overall good agreement with the semi-empirical Lotz formula [17] with inclusion of the 2s and 2p contributions. No theoretical results can be compared to the present results.

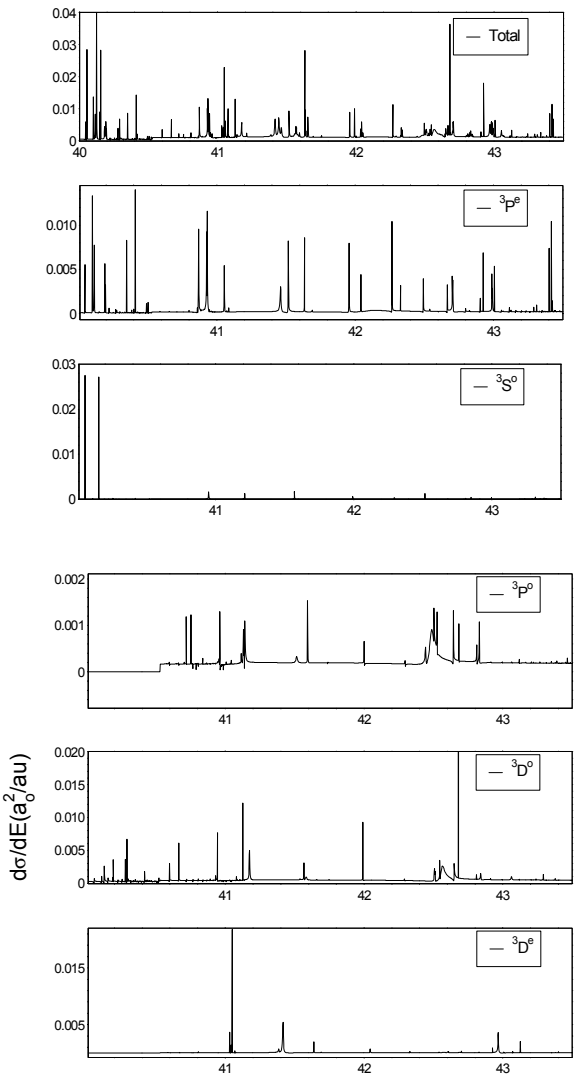

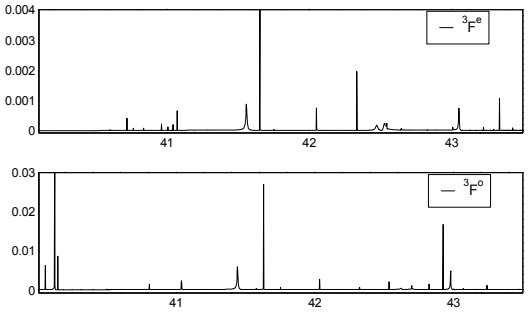

FIG. 1 : Contribution from a particular continuum symmetry to the single differential cross section for ionization of Ar^{10+} by an electron with energy 50 *au* as a function of energy loss. The graph shows a region for energy loss ÄE between the thresholds for producing $Ar^{11+}\,(1s^2 2s^2 2p^3)\ ^4S^o$ and $Ar^{11+}\,(1s^2 2s^2 2p^3)\ ^2P^o$

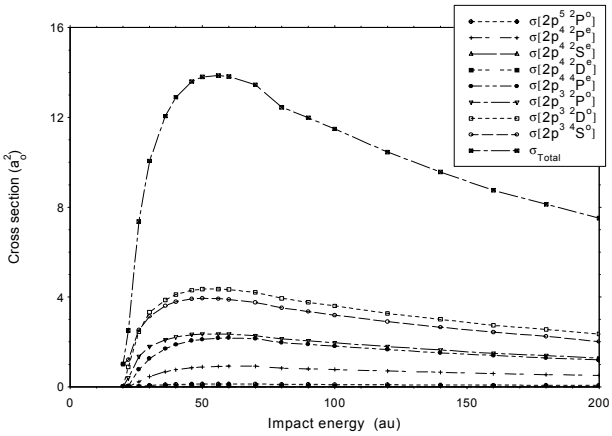

FIG. 2 : Cross sections for electron impact ionization of Ar^{10+}, producing eight states of final Ar^{11+}.

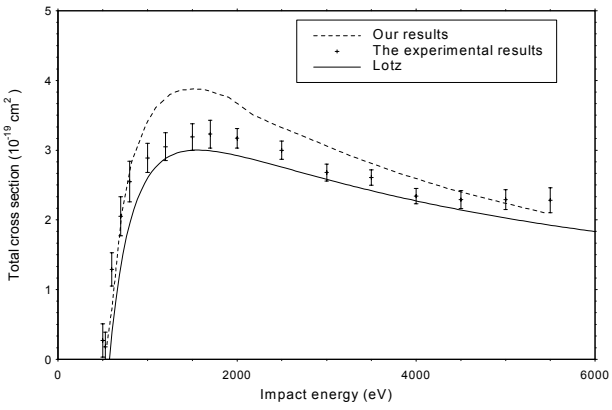

FIG. 3 : Total Cross sections for electron impact ionization of Ar^{10+}, summed over the final states of Ar^{10+}. The results of Defrance and al are also shown (+). The full curve is the semi empirical Lotz formula.

V. CONCLUSIONS

We have calculated total and single differential cross sections for electron impact ionization of Ar^{10+} for a wide range of impact energies, from 20 au (which is just above the threshold energy at 19.8 au) to 200 au. Our calculations has demonstrated the ability of the Bartschat-Burke R-matrix formulation to describe the initial and final state of the ion. The total cross section has a maximum value of $13.86 \times 10^{-3} a_0^2$ at an impact energy of 56 au. Our total cross section, summed over the final states, is in good agreement with the predictions of the semi-empirical Lotz formula and with experimental results [16] . We also calculated total cross section relative to production of each final state of the residual ion, but, we can not compare these results with experimental results. The contribution of autoionization to the total cross section is not significant. These resonances are incorporated automatically by the accurate treatment of the inner region in the R-matrix method. The exchange effects can be included exactly in this formulation and results may be improved significantly in medium impact energy.

Table 1 : The energies used in our ionization calculation, $I(^{2s+1} L_f)$ are relative to the ground state of Ar^{10+}.

Adopted states	Energy $I(^{2s+1} L_f)$ (au)
$1s^2 2s^2 2p^3\ ^4S^o$	19.8058916
$1s^2 2s^2 2p^3\ ^2D^o$	20.2647416
$1s^2 2s^2 2p^3\ ^2P^o$	20.5706516
$1s^2 2s 2p^4\ ^4P^e$	21.7731016
$1s^2 2s 2p^4\ ^2D^e$	22.5579160
$1s^2 2s 2p^4\ ^2S^e$	23.0168316
$1s^2 2s 2p^4\ ^2P^e$	23.2100016
$1s^2 2p^5\ ^2P^o$	25.1428916

Table 2 : Details of autoionization states of Ar^{10+}. The energies are relative to the ground state $Ar^{10+}(1s^2 2s^2 2p^4)^3P^e$. They are given as *I* in Table 1

$Ar^{(10+)}$ symmetry	Energy (Ryd)	$Ar^{(11+)}$ cores	n^*_{min}
$^3P^e$	39.6625	$^2P^o$ 9p	9.0456
	39.6889	$^2D^o$ 12p	12.0371
	39.7926	$^2D^o$ 12f	12.3137
	39.8787	$^4P^e$ 6s	5.7439
	40.1135	$^4P^e$ 6d	5.9337
$^3S^o$	39.6825	$^2D^o$ 12d	11.9529
	39.9772	$^4P^e$ 6p	5.8226
	39.9877	$^2P^o$ 10p	10.2415
$^3P^o$	40.5765	$^2P^o$ 15s	14.6367
	40.5968	$^2P^o$ 15d	14.9071
	40.9605	$^4P^e$ 7p	6.8407
	41.5147	$^2D^e$ 6p	5.7965
	41.5918	$^2D^e$ 6f	5.8596
	41.7383	$^1P^o$ 5p	5.3075
$^3D^o$	39.6439	$^2D^o$ 12g	11.6895
	39.6792	$^2D^o$ 12s	11.6895
	39.7778	$^2D^o$ 13d	12.6873
	39.9115	$^2P^o$ 10p	9.9192
	39.9674	$^4P^e$ 6p	5.8146
	40.1884	$^4P^e$ 6f	6.0029
	40.2662	$^2D^e$5p	4.9949
	40.2998	$^2D^e$ 5f	5.0121
$^3D^e$	40.5859	$^2P^o$ 15p	14.7587
	40.6031	$^2P^o$ 15f	14.9969
	41.0534	$^4P^e$ 7d	6.9670
	41.6895	$^2D^e$ 6s	5.9426
$^3F^e$	40.6013	$^2P^o$ 15f	14.9690
	41.5568	$^4P^e$ 8d	7.7988
	41.6532	$^4P^e$ 8g	7.9945
	41.7528	$^2D^e$ 6d	5.9983
	42.4762	$^2D^e$ 7g	6.7705
$^3F^o$	39.6476	$^2D^o$ 9d	9.0003
	39.6606	$^2D^o$ 12d	11.8013
	39.6606	$^2P^o$ 12d	11.9969
	40.1882	$^2P^o$ 11g	11.0525
$^3G^o$	36.011391	$^2D^o$ 12d	4.9990
	37.234042	$^2P^o$ 10g	5.9987
	37.234042	$^4P^e$ 7f	5.9987
	37.785026	$^2D^e$ 6f	4.9993
$^3G^e$	36.011391	$^4P^e$ 9g	4.9990
	37.234042	$^2D^e$ 6d	5.9987
	37.234042	$^2S^e$ 6g	5.9987
$^3H^e$	41.656601	$^4P^e$ 8g	8.0011

Table 3 : Total cross section for electron-impact ionization of Ar^{10+} with production of Ar^{11+} in various states (columns 3-9). Column 2(Σ) is the cross section summed over the states of Ar^{11+}

Impact energy (au)	Cross section (a_0^2)								
	σ_{Total} $\times10^{-3}$	$\sigma[2p^3\,{}^4S^o]$ $\times10^{-3}$	$\sigma[2p^3\,{}^2D^o]$ $\times10^{-3}$	$\sigma[2p^3\,{}^2P^o]$ $\times10^{-3}$	$\sigma[2p^4\,{}^4P^e]$ $\times10^{-3}$	$\sigma[2p^4\,{}^2D^e]$ $\times10^{-4}$	$\sigma[2p^4\,{}^2S^e]$ $\times10^{-5}$	$\sigma[2p^4\,{}^2P^e]$ $\times10^{-3}$	$\sigma[2p^5\,{}^2P^o]$ $\times10^{-3}$
20	01.0112	1.0112	0.0000	0.0000	0.0000	0.0000	0.0000	0.0000	0.0000
22	02.5164	1.2028	0.8821	0.3972	0.0336	0.0000	0.0000	0.0000	0.0000
26	07.3538	2.5314	2.4570	1.3460	0.7716	0.1195	0.0633	0.0001	0.0127
30	10.0632	3.1453	3.3228	1.7966	1.2558	0.1704	0.1283	0.4533	0.0615
36	12.0538	3.6104	3.8644	2.0899	1.7008	0.1655	0.1531	0.6723	0.0977
40	12.8955	3.7874	4.1082	2.2219	1.8856	0.1709	0.1659	0.7634	0.1099
46	135926	3.9179	4.3022	2.3266	2.0553	0.1750	0.1754	0.8496	0.1215
50	13.8006	3.9441	4.3543	2.3535	2.1192	0.1763	0.1776	0.8840	0.1257
56	13.8675	3.9258	4.3559	2.3557	2.1656	0.1782	0.1768	0.9119	0.1275
60	13.8175	3.8931	4.3353	2.3462	2.1756	0.1795	0.1749	0.9200	0.1273
70	13.4520	3.7590	4.2051	2.2794	2.1488	0.1790	0.1673	0.9155	0.1243
80	125439	3.5175	3.9432	2.1441	1.9676	0.1859	0.1534	0.8364	0.1152
90	11.9871	3.3519	3.7637	2.0487	1.8891	0.1836	0.1445	0.8044	0.1098
100	11.4826	3.1961	3.6029	1.9632	1.8178	0.2377	0.3143	0.7706	0.1045
120	10.4528	2.9060	3.2707	1.7963	1.6580	0.2067	0.1214	0.7050	0.0948
140	095660	2.6545	3.0056	1.6416	1.5158	0.1513	0.2285	0.6445	0.0864
160	08.7524	2.4336	2.7407	1.4886	1.3961	0.1971	0.1000	0.5909	0.0788
180	08.1286	2.2526	2.5573	1.3988	1.2860	0.1321	0.0915	0.5466	0.0725
200	07.5181	20.1024	2.3533	1.2747	1.1995	0.1038	0.0863	0.5089	0.0676

[1] Mark TD 1992 Plasma Phys.Control.Fusion **34** 2083

[2] M.F.A. Harrison, `` The plasma boundary region and the role of Atomic and Molecular Processes '' in Atomic and Molecular Physics of Control Thermonuclear Fusion, ed. C.J. Joachain and D.E. Post, NATO Advanced Study Institue Series B : Physics, vol. 101(Plenum, new York and London, 1983) , pp. 173-474.

[3] Rudge MRH 1968 Rev.Mod.Phys.**40** 564

[4] Defrance P,Duponcelle M and Moores DL 1995 Atomic and Molecular Processes in fusion Edge Plasmas ed RK Janev (New york:plenum) p 153

[5] Bartschat K and Burke PG 1987 J.Phys.B.At.Mol.Phys.**20** 3191

[6] Jakubowicz H and Moores DL 1981 J.Phys.B At.Mol.Phys .**14** 3733

[7] Bartschat K 1993 Compt.Phys.Commun **17** 219

[8] Burke PG, Hibbert A and Robb WD 1971 J.Phys. B :At. Mol. Phys. **4** 153

[9] Burke PG and Robb WD 1975 Adv.At.Mol.Phys.**11** 143

[10] Raeker A, Bartschat K and Reid R H G 1994 J. Phys. B : At. Mol.Opt. Phys. **27** 3129

[11] Reid R H G, bartschat K and Burke P G 1992 J. Phys. B :At. Mol. Opt. Pys. **25** 3175

[12] Laghdas K, Reid R H G, Joachain C J and Burke P G 1995 J ; Phys. B : At. Mol. Opt. Phys. **28** 4811

[13] Clementi E and Roetti C1974 At.Data.tables **14** 270

[14] Hibbert A 1975 Comput.Phys.Commun.**9**.14

[15] Moores D L and reed K J 1994 Adv ; At. Mol. Phys. **34** 301

[16] Defrance P, and al 1999 Private communication.

[17] Lotz W 1967 Astrophys. J Suppl. **14** 207